View metadata, citation and similar papers at core.ac.uk

brought to you by CORE

provided by Digital.CSIC

Morphological and interaction effects on the surface plasmon resonance of metal nanoparticles

This article has been downloaded from IOPscience. Please scroll down to see the full text article.

2003 J. Phys.: Condens. Matter 15 S3001

(http://iopscience.iop.org/0953-8984/15/42/002)

View the table of contents for this issue, or go to the journal homepage for more

Download details:
IP Address: 161.111.22.141
The article was downloaded on 12/12/2012 at 11:27

Please note that terms and conditions apply.

INSTITUTE OF PHYSICS PUBLISHING JOURNAL OF PHYSICS: CONDENSED MATTER

J. Phys.: Condens. Matter **15** (2003) S3001–S3010 PII: S0953-8984(03)63027-4

Morphological and interaction effects on the surface plasmon resonance of metal nanoparticles

J Gonzalo, R Serna, J Solís, D Babonneau[1] and C N Afonso

Instituto de Óptica, CSIC, Serrano 121, 28006 Madrid, Spain

E-mail: cnafonso@io.cfmac.csic.es

Received 30 April 2003
Published 10 October 2003
Online at stacks.iop.org/JPhysCM/15/S3001

Abstract

The influence of the morphology and separation of Ag nanoparticles (NPs) on the position of the surface plasmon resonance has been studied. The NPs have been produced on amorphous a-Al_2O_3 surfaces by means of alternate pulsed laser deposition in a layered structure. The films finally produced consist of five layers containing the NPs with spacing layers of a-Al_2O_3, the space between the NPs also being filled-in with a-Al_2O_3. The in-plane dimensions of the NPs have been varied in the 2–12 nm range while their shape changes from that of spheres to that of oblate ellipsoids. The in-depth separation of the layers containing the NPs was varied in the 8–33 nm range. Above an average in-plane dimension threshold of 4.6 nm, the optical absorption of these nanostructured films exhibits two resonances that shift red and blue in respect to that observed in smaller NPs. The results clearly show that this threshold is well above that at which the NPs become oblate spheroids and it is instead close to the threshold for in-plane coalescence among adjacent NPs. The results also show that multipolar electromagnetic interactions among NPs can be neglected for separations larger than 4.4 ± 0.7 nm but they become important for coalesced NPs.

Introduction

The properties of metal nanoparticles (NPs), often referred to as clusters, colloids or nanocrystals, have widely been studied and analysed with a certain degree of success in the framework of Mie scattering theory. These NPs have attracted recent renewed interest related to, on the one hand, the development of synthesis and characterization techniques that have made possible the control of the features of NPs to within a few nanometres. On the other hand, they show special properties interesting for catalysis, tunnel resonance resistors or optical

[1] Present address: LMP, UMR 6630 du CNRS, UFR Sciences, Bâtiment SP2MI, Bd 3 Téléport 2, 86960 Futuroscope Cedex, France.

0953-8984/03/423001+10$30.00 © 2003 IOP Publishing Ltd Printed in the UK

applications such as selective solar or molecular absorbers, broadband polarizers or all-optical switches.

The optical properties of the NPs are characterized by the surface plasmon resonance (SPR) whose position, width and amplitude depend on the nature of the NPs. These features are also found to change when the NPs are supported on a substrate or embedded in a matrix [1], experience electromagnetic interactions [2] or when the dimensions or shape of the NPs are modified [3]. Ag NPs constitute the most thoroughly studied system because the SPR appears at a wavelength well separated from the interband absorption edge and thus the evolution of its features as a function of those of the NPs and their environment can more easily be analysed. It has been widely reported that the SPR of Ag NPs either supported [3–6] or embedded in a matrix [3, 7, 8] shifts red with respect to that of small NPs as the dimensions of the NPs increase. This SPR will be referred to from now on as the red SPR.

A second resonance has, in some cases, been reported. It is usually observed for NPs bigger than a threshold and to shift blue as the dimensions of the NPs increase [4–6]. It will be referred to from now on as the blue SPR. This resonance is more clearly resolved when using oblique incidence and p-polarization. Thus it has been associated with modes excited when the electrical field vector is perpendicular to the substrate, whereas the red SPR is observed for any NPs' dimensions and independently of the polarization or angle of incidence used. The blue resonance is thus typically associated to the deformation [5, 6] or the non-spherical shape [4] of small NPs (dimensions < 20 nm). However, studies performed in well organized two-dimensional arrays of Ag NPs have attributed the blue SPR to collective effects related to interactions among NPs [9]. Furthermore, recent studies on colloidal NPs of various shapes (with circular, pentagonal and triangular sections) found only the red SPR whose position depended strongly on the NPs' shape [10].

Assuming that the shift in the SPR is related to changes in the NPs shape, their height (i.e. dimension in the direction perpendicular to the substrate)—that is, a magnitude usually difficult to measure experimentally—has been determined from the fit of the experimental absorption spectra [4–6]. Nevertheless, this approach is only considered valid if the NPs are well separated so they can be treated as isolated NPs on a substrate, thus limiting the analysis to very small NPs [5]. An alternative interpretation, based on multipolar interaction among the NPs, is claimed to be responsible for the shift of the SPR observed for embedded NPs produced by ion implantation [2] that are most likely spherical. All the above-mentioned studies used either the average dimensions determined by plan-view images obtained by transmission electron microscopy (TEM) [2, 4, 5] or the NPs' density obtained by scanning force microscopy (SFM) to discuss the features of the SPRs [6]. Therefore, the absorption spectra have not yet been analysed in terms of experimentally determined NPs' heights and thus the validity of these models and the range of separations for which the isolated particle approximation is valid have not yet been determined experimentally. The aim of this work is to bring new insights into the dependence of the optical absorption spectra on the features of Ag NPs. It involves not only the experimental determination of the in-plane average dimensions, the heights and separation of the NPs, but also the variation of the NPs' separations in a controlled way to determine the range in which particle–particle interactions can be considered negligible.

Experimental details

Ag NPs are embedded in an amorphous a-Al_2O_3 matrix by pulsed laser deposition in vacuum (10^{-6} mbar), thus forming a nanocomposite of Ag:Al_2O_3. An ArF excimer laser beam ($\lambda = 193$ nm, $\tau = 20$ ns FWHM) operating at 10 Hz has alternately been focused on the surface of high purity Al_2O_3 and Ag targets at an angle of incidence of 45°. The targets

Table 1. Ag areal density per layer [Ag], in-depth NP separation and total thickness of the Ag:Al_2O_3 nanocomposite films studied in this work.

[Ag] ($\times 10^{15}$ atom cm^{-2})	In-depth NP separation (nm)	Film thickness (nm)
0.5	25 ± 2	150 ± 6
0.6	25 ± 2	150 ± 6
0.7	20 ± 2	118 ± 6
1.0	25 ± 2	150 ± 6
1.4	21 ± 2	125 ± 6
2.8	21 ± 2	131 ± 6
3.8	21 ± 2	132 ± 6
4.0	25 ± 2	150 ± 6
5.2	22 ± 2	140 ± 6
6.3	25 ± 2	140 ± 6
7.1	22 ± 2	141 ± 6
9.7	22 ± 2	143 ± 6
12.4	22 ± 2	145 ± 6
2.5	8 ± 2	168 ± 8
2.5	10 ± 2	186 ± 9
2.5	22 ± 2	185 ± 9
2.4	33 ± 2	178 ± 8

were mounted in a computer-controlled holder that allows both the continuous rotation and the sequential ablation of the targets. An average energy density of $\approx$2 J cm^{-2} has been used to ablate both targets. The resulting Ag:Al_2O_3 films were grown at room temperature on Si and fused silica substrates placed 32 mm away from the target surface.

The deposition rates of both the matrix and the metal are independently determined in vacuum prior to the production of the nanocomposite by means of *in situ* reflectivity measurements. An amorphous a-Al_2O_3 layer is deposited first so the Ag NPs nucleate always on the same type of surface. Once the NPs are produced and distributed on this surface, the matrix target is ablated to first fill-in the space among the NPs and, second, produce an a-Al_2O_3 layer with a certain thickness and a flat surface [11]. This sequence has been repeated five times (the desired number of Ag NP layers) and therefore the films are always finished by an a-Al_2O_3 protective layer. Further details of the synthesis procedure of these nanocomposite films, as well as their structure as analysed by TEM, can be found elsewhere [12].

The areal density of Ag atoms per layer [Ag], the film thickness and the in-depth separation between NP layers have been determined by Rutherford backscattering spectrometry (RBS) on the films deposited on Si substrates as described elsewhere [12, 13]. These data are summarized in table 1 for all the films studied in this work. Two series of specimens have been studied:

(i) a series in which [Ag] is increased (and consequently the dimensions of the NPs are increased) while the in-depth separation is kept approximately constant; and
(ii) a series in which the in-depth separation of the NPs is varied in the range 8–33 nm while [Ag] is kept approximately constant.

To keep the total film thickness constant in the latter series, the thickness of the protective a-Al_2O_3 layer (i.e. the last one deposited that is at the surface) was increased as the in-depth separation was decreased.

The average in-plane dimensions of the NPs as well as their height (in the direction perpendicular to the substrate) have been determined by grazing incidence small angle x-ray

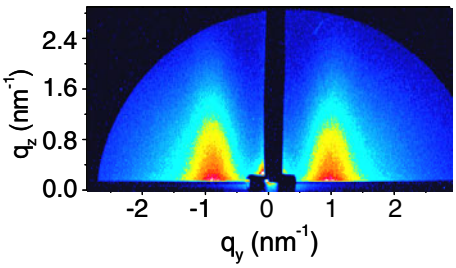

Figure 1. GISAXS pattern obtained in the Ag:Al_2O_3 film grown on Si with [Ag] = 2.5×10^{15} atom cm^{-2}.

(This figure is in colour only in the electronic version)

scattering (GISAXS) on the films deposited on Si substrates. The energy was set to 9000 eV, corresponding to a wavelength of 0.138 nm. The distance between the sample and the detector was 700 mm and the angle of incidence was slightly higher than the critical angle of the films ($\alpha \approx 0.22°$) in order to penetrate into the layer [14].

Finally, the optical absorption spectra α of the nanocomposite films deposited on fused silica substrates have been determined as $\alpha = -(\ln \mathrm{T})/d$, where d is the total film thickness determined by RBS and T is the transmission measured under ambient conditions using a WVASE J A Woollam ellipsometer. The light beam was p-polarized and the angle of incidence has been varied with respect to the surface normal of the film from 0° to 70°. The photon energies ranged from $E = 1.5$ to 4.5 eV with a spectral resolution of $\Delta E = 20$ meV. All the measurements were corrected for the spectral emission profile of the lamp, the wavelength-dependent transmission of the optical components and the spectral response of the photodiodes. A bare fused silica substrate was used to rule out any contribution from the substrate.

Results

Figure 1 shows a typical GISAXS pattern obtained from a Ag:Al_2O_3 film. An intense scattering signal is observed on either side of the vertical beam stop with an interference maximum in the direction parallel to the surface. The existence of clear and well defined peaks shows the presence of scattering NPs with defined sizes of a few nanometres. The angular position of the intensity maximum $q_{\max}$ along the horizontal axis gives the value of the mean centre-to-centre separation of the NPs as $2\pi/q_{\max}$. The lateral and vertical extensions of the scattering yield provide the average lateral and vertical dimensions of the NPs, i.e. their average in-plane diameter $\langle \varnothing \rangle$ and mean height $\langle H \rangle$, respectively [14]. Films having [Ag] $< 1.0 \times 10^{15}$ atom cm^{-2} showed no GISAXS pattern either because the dimensions of the NPs were below the resolution limit or because they were not yet formed.

Figure 2(a) shows that both $\langle \varnothing \rangle$ and $\langle H \rangle$ increase as a function of the metal content per layer up to values close to 5 nm after which $\langle \varnothing \rangle$ continues growing while $\langle H \rangle$ remains nearly constant. The smallest NPs detected exhibit $\langle H \rangle \approx \langle \varnothing \rangle \approx 2$ nm and thus they can be considered as spherical. Otherwise, $\langle H \rangle$ is always smaller than $\langle \varnothing \rangle$, thus indicating the NPs become oblate spheroids with the shorter axis being perpendicular to the film surface. It is worth pointing out that these results are consistent with those reported earlier that were extracted from plan-view TEM images [12]. The minimum dimensions detectable by TEM were 1.1 nm for [Ag] $= 0.7 \times 10^{15}$ atom cm^{-2} and the NPs were seen as spherical for average diameters <4 nm or [Ag] $< 4 \times 10^{15}$ atom cm^{-2}. For [Ag] $\geqslant 6 \times 10^{15}$ atom cm^{-2},

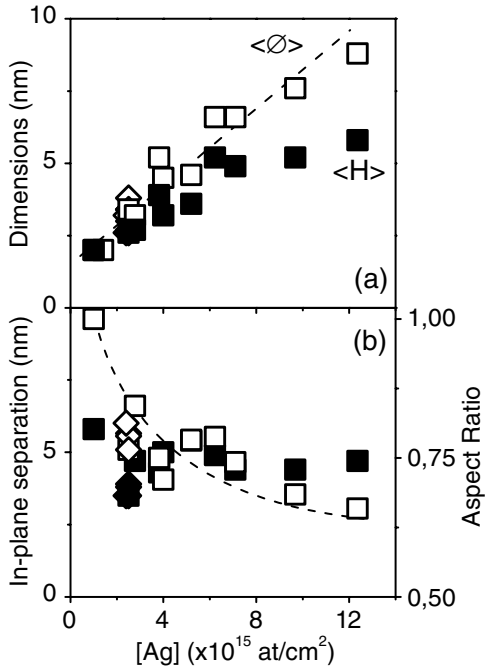

Figure 2. Features of the Ag NPs as determined from the GISAXS patterns as a function of [Ag]: (a) (□, ◇) in-plane average diameter $\langle\varnothing\rangle$, (■, ♦) mean height in the direction perpendicular to the film plane $\langle H\rangle$; (b) (■, ♦) mean in-plane surface-to-surface separation and (□, ◇) effective aspect ratio $\langle H\rangle/\langle\varnothing\rangle$. The data correspond to the series of films in which (□, ■) [Ag] and (♦, ◇) in-depth separation have been varied.

coalescence was found to occur and NPs with average in-plane diameters >6 nm become elongated in the plane, the average in-plane dimensions measured here by GISAXS being in very good agreement with the average length and breadth reported earlier. Figure 2(b) shows the evolution of the surface-to-surface in-plane NPs separation defined as the centre-to-centre separation minus $\langle\varnothing\rangle$, and the effective aspect ratio calculated as $\langle H\rangle/\langle\varnothing\rangle$ both as a function of [Ag]. Whereas the former is found to remain approximately constant around 4.4 ± 0.7 nm, the latter is found to decrease as [Ag] increases.

Figure 3 shows the optical absorption spectra for the film having [Ag] $= 12.4 \times 10^{15}$ atom cm^{-2} and $\langle\varnothing\rangle = 8.8$ nm measured at different incidence angles. At normal incidence, a single absorption resonance peaking at 2.42 eV is observed, that is most likely related to the red SPR. A second resonance appears at 3.68 eV whose intensity increases as the of angle of incidence is increased, that most likely corresponds to the blue SPR. In order to study the dependence of the features of these two resonances on the morphology and distribution of the NPs, the optical spectra presented from now on have all been measured at 45° since the contributions of both modes are well resolved at this angle. This selection will also ease the comparison with earlier reported results in which a similar configuration has been used [5, 6].

Figure 4 shows the absorption spectra of some selected films of the first series of specimens prepared with increasing in-plane dimensions of the NPs while keeping constant their in-depth separation. All the spectra exhibit the red SPR whose intensity increases and position shifts red as $\langle\varnothing\rangle$ increases. The lowest [Ag] for which the red SPR is observed is [Ag] $= 1.0 \times 10^{15}$ atom cm^{-2}, this result being consistent with those obtained by GISAXS,

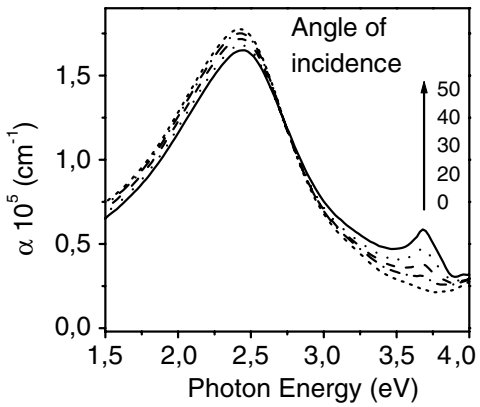

Figure 3. Absorption spectra of a specimen having [Ag] $= 12.4 \times 10^{15}$ atom cm^{-2}, $\langle\varnothing\rangle = 8.8$ nm and in-depth NPs' separation of 22 nm as a function of the angle of incidence (values given in degrees in the figure).

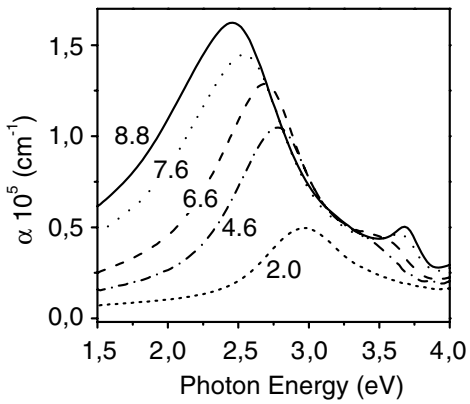

Figure 4. Absorption spectra of specimens having increasing $\langle\varnothing\rangle$ (values given in nanometres in the figure) and having constant in-depth NPs' separation of $\approx$22 nm.

thus confirming that the minimum dimension detectable by both techniques is $\approx$2 nm. When comparing the absorption spectra obtained for this specimen to that measured earlier by ellipsometry for the same specimen in which no SPR could be detected [13], it is clearly observed that the resolution of the present absorption spectra is higher than that of the earlier ellipsometry measurements. The reasons for the improved resolution of the present measurements are most likely related to the more favourable angle of incidence used in this work together with the use of the appropriate light polarization.

The blue SPR is first visible for the specimen having [Ag] $= 5.2 \times 10^{15}$ atom cm^{-2} for which $\langle\varnothing\rangle = 4.6$ nm. Its intensity increases and its position shifts blue as $\langle\varnothing\rangle$ is further increased. The series of specimens prepared at constant [Ag] and changing in-depth separation had $\langle\varnothing\rangle = 3.4 \pm 0.3$ nm, that is a value below the threshold for the blue SPR, and thus they only exhibit the red SPR as shown in figure 5. This figure also shows that the features of the resonance do not depend significantly on the in-depth separation of the NPs in the range studied.

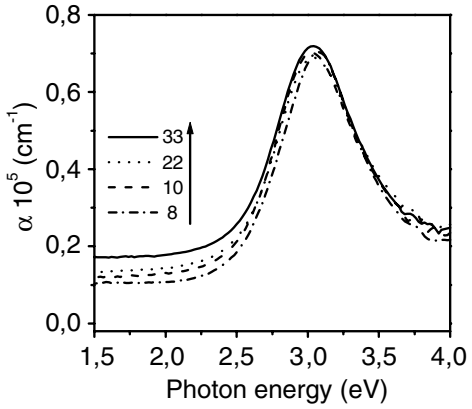

Figure 5. Absorption spectra of specimens having $\langle \varnothing \rangle = 3.4 \pm 0.3$ nm and increasing in-depth NPs' separations (values given in nanometres in the figure).

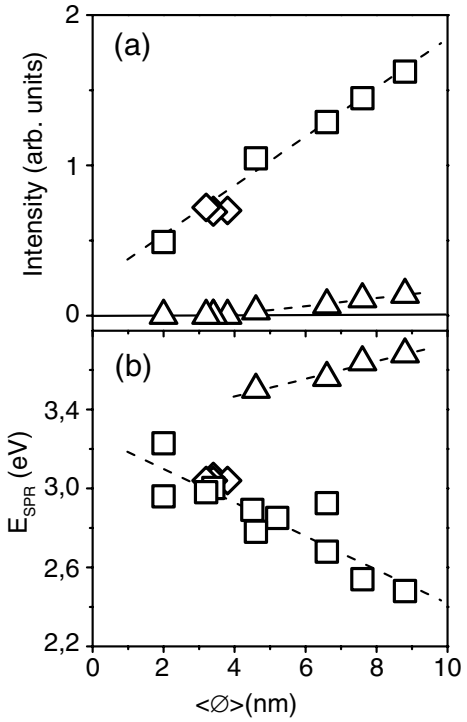

Figure 6. (a) Intensity and (b) position of the (□, ◇) red and (△) blue SPRs as a function of the in-plane diameter $\langle \varnothing \rangle$ of the NPs. (◇) correspond to the results achieved in the second series of films in which the in-depth NPs' separation has been varied. The lines are linear fits.

The position of both SPRs as a function of the most relevant features of the NPs are plotted in figures 6–8. Figure 6 shows that the (a) intensity and (b) position of the SPRs follow a linear dependence on the average in-plane diameter. Figure 7 shows the dependence of the position of the SPRs on the NPs' aspect ratio. Finally, the position of the SPRs are plotted as a function of the NPs' surface-to-surface separation both in-plane and in-depth in figure 8. It is clearly

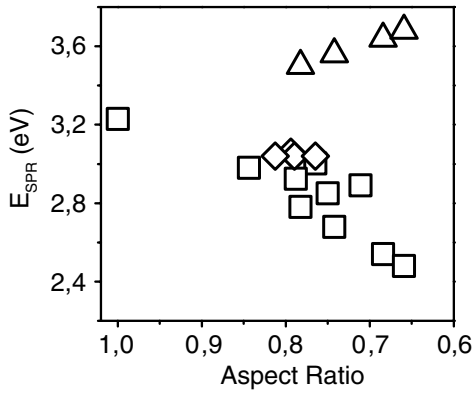

Figure 7. Position of the (□, ◇) red and (△) blue SPRs as a function of the aspect ratio $\langle H \rangle / \langle \varnothing \rangle$ of the NPs. (◇) correspond to the results achieved in the second series of films in which the in-depth NPs' separation has been varied.

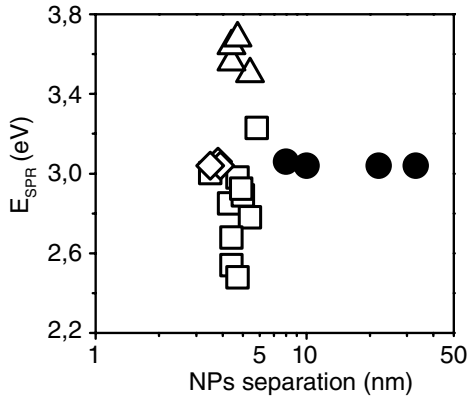

Figure 8. Position of the (□, ◇, ●) red and (△) blue SPRs as a function of the (□, ◇, △) in-plane and (●) in-depth NP separation. (◇, ●) correspond to the results achieved in the second series of films in which the in-depth NP separation has been varied.

seen that the red SPR does not shift when changing the in-depth separation (and thus keeping the dimensions constant) while both the blue and red SPRs shift when the in-plane separation is kept constant but the dimensions and aspect ratio change (as shown in figures 6 and 7).

Discussion

Electromagnetic interactions among NPs are known to lead to complex extinction spectra by splitting the resonances and thus making it difficult to separate their role on the features of the SPR from that of the shape [15, 16]. They are considered to be effective for NP separations smaller than 5 times the NPs' radius, this value being varied in the present work from 5 nm for the smallest NPs to 22 nm for the largest ones. Since the in-plane NPs' separations considered in this work satisfy in all cases this condition, it would imply that the optical response of the NPs should be dominated by electromagnetic interactions in all cases. However, the results plotted in figure 8 clearly show that the red SPR does not change its position when changing the separation of the NPs. This allows us to conclude that the electromagnetic coupling can be

neglected for NPs' separations larger than 4.4 ± 0.7 nm, independent of the NPs' dimensions or shape. This conclusion also questions the appropriateness of the above-mentioned modelling to describe the interaction between neighbouring NPs.

Assuming that the NPs interactions can be neglected, the splitting and shift of the SPRs have mainly been discussed in terms of the non-spherical shape of the NPs caused by the deformation induced by the substrate [5, 6]. Using this approach, the height of the NPs is extracted from simulation of the optical spectra leading to aspect ratios close to 0.4 for NPs with mean diameter >8 nm [6]. The aspect ratio obtained experimentally in this work for this mean diameter is much higher (0.68, see figure 2) although the technique used here (PLD) involves species that are at least two orders of magnitude more energetic than those involved in the thermal evaporation process used elsewhere. Thus the deformation would be expected to be higher in the present experimental conditions. Furthermore, it is worth noting that the appearance of the blue SPR does not relate directly to the oblate spheroidal shape of the NPs, as can be appreciated in figures 6 and 7 where it is clearly seen that there are several specimens containing non-spherical NPs for which their absorption spectra do not show the blue SPR. As an example, the specimens whose absorption spectra are plotted in figure 5 show no blue SPR although they have NPs with dimensions around 3.4 nm and an aspect ratio of 0.79 ± 0.02.

Regarding the influence of the shape in the splitting of the SPR into red and blue, the results obtained by TEM in similar specimens reported earlier show that the in-plane NPs' shape becomes elongated for [Ag] $\geqslant 6 \times 10^{15}$ atom cm^{-2} [12]. According to figure 2, this value corresponds to average in-plane dimensions close to 5 nm and the specimen indeed shows the blue SPR as shown in figure 4. Nevertheless, these NPs have a similar aspect ratio than those having dimensions around 3.4 nm, and thus are approximately round in plane and do not exhibit the blue SPR (figure 5). It can be then concluded that the appearance of the blue SPR is not directly related to the NPs being oblate spheroids with their short axis in the direction perpendicular to the substrate. Instead, the blue SPR appears clearly once coalescence of neighbouring NPs starts and thus many NPs exhibit in-plane elongated shapes that differ from the circular one assumed so far as shown in figure 2 of [12]. The shape of these coalesced NPs becomes close to that of oblate *ellipsoids* in which the short in-plane axis is only slightly higher than the short out-of-plane axis. Our results are consistent with those reported elsewhere for Ag NPs on quartz–glass substrates, in which the simulation of the absorption spectra for films having a certain degree of coalescence could not be achieved by assuming rotationally symmetric oblate spheroids [4]. They are also very much consistent with those reported earlier for NPs of different shapes in which only one resonance was observed [10].

Although the reasons for this behaviour are not clear at this point, it is possible that these coalesced NPs do not behave from the optical point of view as single NPs but as two (or several) NPs extremely close to each other and thus electromagnetic coupling between these *contacting* NPs becomes important. This reasoning is consistent with the results achieved for Ag NPs produced by ion implantation into crystalline SiO_2 [2]. With this technique, the NPs are nucleated by the defects produced by ion implantation and thus the embedded NPs are expected to be spherical as opposed to what happens when using deposition techniques in which the substrate marks an asymmetry for the growth process of supported NPs. The shift observed in the SPRs was discussed in terms of multipolar interactions among the NPs that are very close to each other due to the extremely high metal concentration. Our results are also very much in agreement with the results reported elsewhere for assembled coupled Ag particle dimers for which the splitting of the SPR is observed for separations of 2 nm but not for separations of 6 nm [17]. They might also be related to the onset of quantum mechanical coupling between adjacent NPs that has been reported to occur when the NPs' separation is reduced below 1.2 nm [18]. We can thus conclude, in agreement with some of the earlier

reports [2, 17, 18], that electromagnetic multipolar interactions among *contacting* and adjacent NPs above the coalescence threshold are responsible for the splitting of the SPR rather than their oblate spheroid shape that appears as a consequence of their growth on a substrate.

Conclusions

Ag NPs produced on an amorphous Al_2O_3 surface show two optical absorption resonances whose maxima separate as the dimensions of the NPs increase for in-plane average dimensions above a threshold value of 4.6 nm. Below this threshold, only one resonance is observed and the NPs can generally be considered as oblate *spheroids* with their short axis perpendicular to the substrate (except for the smallest NPs detected in this work that can be considered as 2 nm diameter spheres). Above this threshold, the NPs acquire irregular shapes due to coalescence of neighbouring particles, most of them having a shape close to oblate *ellipsoids* with the long axis lying parallel to the substrate. In view of these results and since the position of the SPRs does not depend on the NPs' separation, it is concluded, on the one hand, that multipolar electromagnetic interactions among NPs can be neglected for NPs' surface-to-surface separations $\geqslant 4.4 \pm 0.7$ nm, independent of the dimensions or shape of the NPs. On the other hand, we conclude that the splitting of the SPR into red and blue components is associated with multipolar electromagnetic interactions among *contacting* NPs that appear once coalescence starts.

Acknowledgments

This work has been partially supported by MCYT under project TIC2002-03235 and EU under HPRNCT-2002-00328. DB acknowledges a Marie Curie Fellow grant from EU (HPMF-CT-2000-00736). We are grateful to the technical staff of LURE-DCI for providing the synchrotron beam and for assistance during the GISAXS experiment.

References

[1] Hilger A, Tenfelde M and Kreibig U 2001 *Appl. Phys.* B **73** 361
[2] Liu Z, Wang H, Li H and Wang X 1998 *Appl. Phys. Lett.* **72** 1823
[3] Kreibig U and Genzel L 1985 *Surf. Sci.* **156** 678
[4] Singer R R, Leitner A and Aussenegg F R 1995 *J. Opt. Soc. Am.* B **12** 220
[5] Hövel H, Hilber A, Nusch I and Kreibig U 1997 *Z. Phys.* D **42** 203
[6] Stietz F and Träger F 1999 *Phil. Mag.* B **79** 1281
[7] Uchida K, Kaneko S, Omi S, Hata C, Tanji H, Asahara Y, Ikushima A J, Tokizaki T and Nakamura A 1994 *J. Opt. Soc. Am.* B **11** 1236
[8] Banerjee S and Chakravorty D 1998 *Appl. Phys. Lett.* **72** 1027
[9] Taleb Al, Russier V, Courty A and Pileni M P 1999 *Phys. Rev.* B **59** 13350
[10] Mock J J, Barbic M, Smith D R, Schultz D A and Schultz S 2002 *J. Chem. Phys.* **116** 6755
[11] Serna R, Afonso C N, Ricolleau C, Wang Y, Zheng Y, Gandais M and Vickridge I 2000 *Appl. Phys.* A **71** 583
[12] Barnes J-P, Petford-Long A K, Coole R C, Serna R, Gonzalo J, Súarez-García A, Afonso C N and Hole D 2002 *Nanotechnology* **13** 465
[13] de Sande J C G, Serna R, Gonzalo J, Afonso C N, Hole D E and Naudon A 2002 *J. Appl. Phys.* **91** 1536
[14] Naudon A and Thiaudiere D 1997 *J. Appl. Crystallogr.* **30** 822
[15] Kreibig U and Vollmer M 1995 *Optical Properties of Metal Clusters* (*Springer Series in Material Science vol 25*) (Heidelberg: Springer)
[16] Gérardy J M and Ausloos M 1982 *Phys. Rev.* B **25** 4204
[17] Novak J P and Feldheim D L 2000 *J. Am. Chem. Soc.* **122** 3979
[18] Collier C P, Saykally R J, Shiang J J, Henrichs S E and Heath J R 1997 *Science* **277** 1978